DESIGN OF A LOW-COMPLEXITY RECEIVER FOR IMPULSE-RADIO ULTRA-WIDEBAND COMMUNICATION SYSTEMS

Chia-Hsiang Yang, Yu-Hsuan Lin, Shih-Chun Lin, Tzi-Dar Chiueh

Graduate Institute of Electronics Engineering
and Department of Electrical Engineering
National Taiwan University, Taipei, Taiwan, 10617

ABSTRACT

In this paper, we propose a low-complexity impulse-radio ultra-wideband (UWB) receiver architecture for short-range communication. Algorithms for pulse position and symbol boundary detection, data despreading and decision as well as timing error tracking are embedded in this receiver. Since hardware simplicity is the main consideration of this design, circuit design issues are taken into account early in the design cycle. Simulation results show that the low-complexity architecture works very well in realistic multipath fading channels.

1. INTRODUCTION

Recently, low-cost, short-range wireless communication applications such as radio frequency identification (RF-ID) and wireless sensor network have received much attention, and impulse-radio UWB is one of the prominent implementations [1][2]. Basically, the impulse-radio UWB communication systems transmit nano-second baseband pulses that spread signal energy over a wide bandwidth, and do so without the up/down converters and frequency recovery loop in conventional passband communication systems. This simpler receiver structure entails lower cost and lower power consumption than existing short-range wireless communication systems. Furthermore, the highly accurate pulse timing in impulse-radio UWB signals makes possible location awareness capability in UWB receivers [3]. With this extra information, several interesting networking technologies have been developed in ad hoc and multi-hop wireless networks.

This paper is organized as follows. In Section 2 we will introduce the impulse-radio technique and the packet format in the proposed UWB system. Next, a receiver architecture based on the packet format is presented in Section 3. Then, Section 4 provides simulation results of this system in multipath fading channels and its implementation. Finally, Section 5 concludes this paper.

This work was supported in part by MediaTek Inc. HsinChu, Taiwan 300.

2. SIGNALING AND PACKET FORMAT

The signal band of impulse-radio UWB signal may overlap with those of many existing narrowband communication systems. Thus, the FCC has limited the usage of the UWB technology by mandating a transmission power spectral density (PSD) mask [4]. Moreover, such band overlay necessitates adopting spread-spectrum techniques in UWB signaling for combating the narrowband interferences. In the proposed UWB system, we choose the direct sequence spread-spectrum (DSSS) technique with bipolar pulse amplitude modulation (PAM). A Golay sequence is chosen as the spreading code for its low-complexity correlator structure [5] and the spreading factor is a power of two that ranges from 1 to 1024. The received pulse waveform is presumably the second derivative of the Gaussian pulse [1] with 4-ns pulse width and 16-ns pulse repetition time. These parameters are selected to make the PSD of the proposed UWB signal comply the FCC limit mentioned above.

Due to the timing-critical nature of the impulse-radio signals, accurate timing must be recovered from the received waveform. Moreover, since the system uses low duty-cycle signal as in [1], three quarters of a pulse repetition interval is nothing but noise and interference. Detecting where the pulses are located is thus by far the first task in the detection of the UWB signal. To this end, the transmitter sends two preambles, regular and coded preambles, at the start of a packet. Fig. 1 shows the proposed physical layer packet format. The regular preamble is made up of a sequence of pulses with alternating signs, with which the receiver detects the pulse position in a pulse repetition interval. After the regular preamble, the coded preamble is for the receiver to detect the start of the data portion in a packet and thus the symbol boundary. A Golay codeword is repeated four times, with the first three Golay-coded preamble symbols sent directly and the last preamble symbol sent with reversed polarity. Each codeword chip is a pulse of proper polarity.

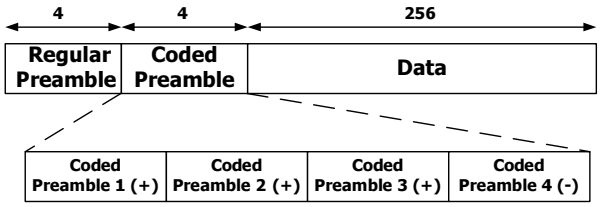

Fig. 1. Proposed physical layer packet format

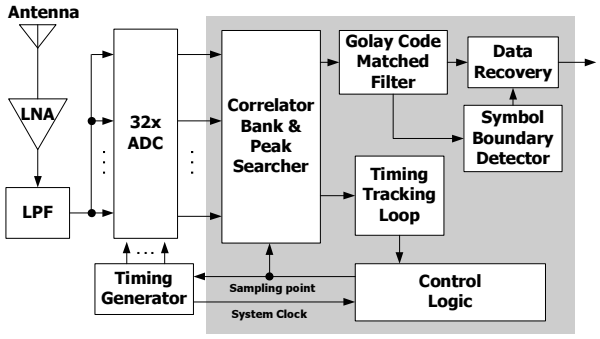

Fig. 2. System block diagram including analog frontend

3. RECEIVER FUNCTION AND ARCHITECTURE

The overall block diagram of the proposed impulse-radio UWB system is depicted in Fig. 2. The received signal first passes through an antenna, a low noise amplifier (LNA), and a low-pass filter (LPF). Then it is sampled by a 32-phase parallel interleaved analog-to-digital converter (ADC) with 2GHz sampling frequency and one-bit resolution, providing 8 samples per pulse. As the design in [2], the UWB system, being noise and interference dominated, is quite insensitive to quantization noises. Therefore, low-resolution analog-to-digital conversion with simple ADC structure is sufficient. The digitized samples are sent to the digital portion of the receiver for further signal processing.

In the receiver, the pulse position synchronization block is always active when searching for a UWB packet. The correlator bank and the peak searcher in Fig. 2 are responsible for this task. After correctly establishing pulse position, symbol boundary synchronization then kicks in through the Golay code matched filter and the symbol boundary detector. With correct pulse and symbol timing, the receiver then detects the received signal using the data recovery block. At the same time, the timing tracking block also operates to maintain the synchronization of the sampling clock. In the subsequent subsections, we will describe the detail function of each block.

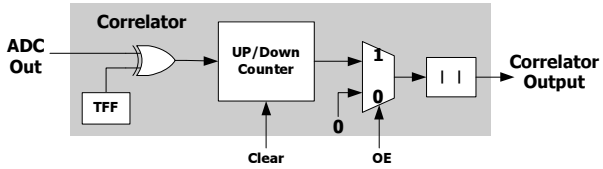

Fig. 3. Block diagram of the proposed correlator.

3.1. Correlator Bank and Peak Searcher

A bank of N_s correlators that are each one sample apart in the time domain are used to accumulate the correlation of the incoming waveform with the pulse waveform over N pulse repetition intervals. In this particular case, $N_s = 32$ and $N = 1024$. Since the pulses in the regular preamble have alternating signs, the pulses are multiplied by '$+1$' or '-1', and the results are accumulated. With coherent integration, one of the correlators will have the largest accumulated correlation output, and the timing of this correlator indicates the pulse position location.

To further minimize complexity, every one of the 32 correlators in the correlator bank is actually a one-tap filter, instead of 8-tap. The one-tap correlator detects the sample position with the highest signal intensities regardless of the received pulse shape. As shown in [6], this one-tap correlator is about 2dB worse than the 8-tap one. The simplified correlator then reduces to one multiplier-and-accumulator (MAC) with $+1/-1$ coefficients, which is furthermore simplified to an up/down counter since the incoming samples are only one-bit wide. This circuit is shown in Fig. 3, where an absolute function operator is used to ensure all correlator outputs are positive. When compared with the correlator in [2] that uses 5-bit coefficients and 128 taps, this correlator requires only a small fraction of hardware resources.

The outputs of the correlator bank are sent to the peak searcher, which then finds the maximum among them and thus determines the pulse position. This maximum value will be compared to a pre-defined threshold to guarantee its legitimacy since if the incoming signal is nothing but noise and interference, the peak found is not likely to exceed the threshold.

3.2. Golay Code Matched Filter

In the proposed system, the length-1024 Golay code replaces the maximal-length PN code used in [2]. A pipelined Golay code matched filter is illustrated in Fig. 4. The code generator of the Golay code has a similar structure except that the delay elements are moved to the other arm. The regular structure makes the adders in the Golay-code matched filter far fewer than those in the PN-code matched filter. For example, the matched filter for a length-1023 PN code needs perform hundreds of additions per sample, while only 20

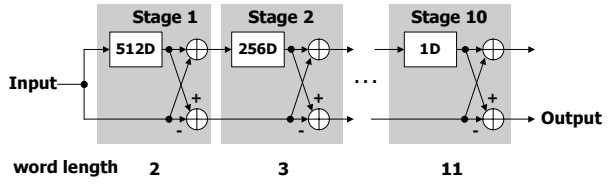

Fig. 4. Block diagram of the pipelined length-1024 Golay code matched filter.

adders are there in a length-1024 Golay-code matched filter. Note that the number of delay elements is halved every stage and the signal word length increases by one each stage. Since more than half of the delay elements have the minimum word length and only one element has the maximum word length, the number of memory elements required in the Golay-code matched filter will be much smaller than other pipelined matched filters.

3.3. Symbol Boundary Detector

During the coded preamble, the Golay-code matched filter will generate peak values for the boundary detector in each preamble symbol. In additive white Gaussian noise (AWGN) channel with acceptable SNR, the indices corresponding to the maximum peak in the coded preamble symbols will not fluctuate by too much. However, in a multipath channel the inter-chip interference (ICI) exists and spurious peaks may be falsely detected. In addition, at low SNR cases, high-intensity noise component in the code matched filter output may also override the true maximum peak and generate a false maximum peak detection. To overcome these difficulties, we record the three largest peaks in three consecutive symbols and their corresponding indices, so on the total there are nine indices and nine peak values. Then the differences between all possible pairs of indices are computed and the minimum distance is compared to a threshold for validity. The index that corresponds to the smallest distance indicates the true peak, with which the symbol boundary can be derived. This algorithm recovers the true symbol boundary buried in the noise in more cases than the other methods that have been tried. The overall symbol boundary detection algorithm is depicted in Fig. 5. Note that a last check for the polarity reversal is necessary to identify the end of the coded preamble.

3.4. Timing Tracking Loop

Clock timing error causes the ADC sampling point to drift. Since the pulses used in the UWB system are very narrow, a small timing error makes the whole receiver out of synchronization. A timing tracking loop is needed to recover the clock timing. In the proposed receiver, we use the early/late

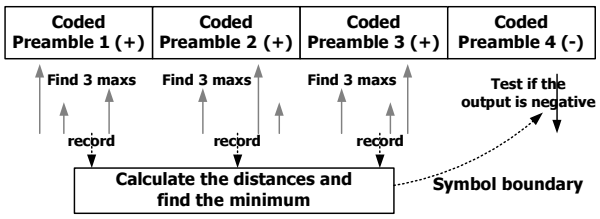

Fig. 5. Symbol boundary detection method in the proposed receiver.

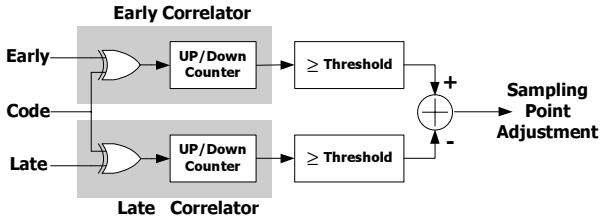

Fig. 6. Block diagram of the early-late timing tracking loop.

timing recovery loop (shown in Fig. 6) that has two correlators. The early and late correlators will correlate the code with two signals, one-sample earlier and one-sample later than the synchronized signal, respectively. With perfect sample timing, the early and late correlators output two positive values of approximate magnitude, keeping the sampling phase essentially unchanged. Nevertheless, drift in sampling point causes either correlator output to fall below the other output, driving the sampling point toward the perfect timing due to the negative feedback nature of the loop.

4. SIMULATION RESULTS AND CHIP IMPLEMENTATION

Before illustrating the simulation results, the channel model used in the simulation is introduced. This model includes the impact of multipath fading, AWGN and timing error. The multipath model is based on the measurement result in [7], obtained from performing propagation experiment in an office. From these data, we generate two channels: typical channel and high-quality channel with root-mean square (RMS) delays of about 20 ns and 10 ns, respectively. The ADC sample timing offset is set to 4 ppm. As mentioned previously, the pulse repetition rate is 62.5 MHz and the Golay code length is 1024, so the data rate is about 61 Kbps.

Fixed-point-arithmetic functional simulation of the proposed impulse-radio receiver under the above channels is then conducted. The fixed-point-arithmetic receiver simulation has a performance that is consistently 2dB worse than the floating-point case. This primarily results from the 1-bit quantization of the ADC. The symbol boundary detection probabilities under two different channels are plotted in

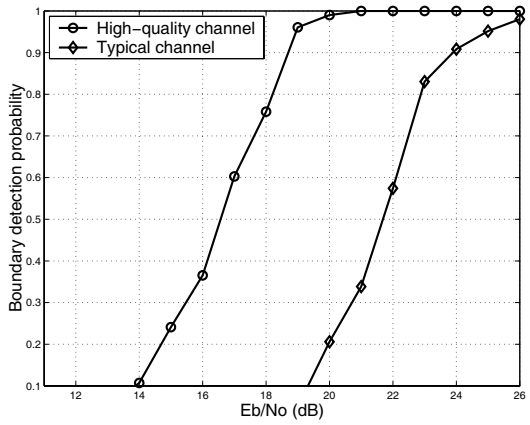

Fig. 7. Fixed-point simulation results of boundary detection probability on two channels.

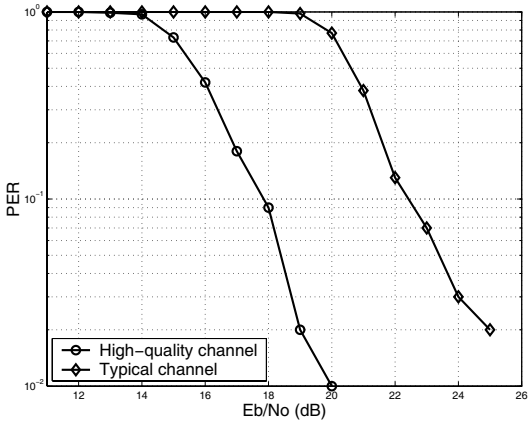

Fig. 8. Simulated impulse-radio UWB system packet error rate using fixed-point arithmetic.

Fig. 7. Furthermore, we assume that a forward error correcting (FEC) code that can correct up to four errors in a packet with 256 bits (each bit is spread to 1024 pulses) is applied. The packet error rate (PER) with such an FEC code is plotted in Fig. 8.

In summary, the high-quality channel case is about 5dB better than the typical-channel case. The performance degradation in boundary detection probability and PER is due to the larger delay spread. Larger delay spread causes more severe ICI and more variations in the channel impulse response, both of which affect the accuracy in boundary detection and therefore PER. Consider a maximum allowable PER of 10% as in the IEEE 802.11 WLAN standard, the proposed UWB system functions well above Eb/N0=22dB. With an enhanced FEC code, the PER performance can be further improved, albeit at a cost of reduction in data rate.

We have described the above UWB transceiver architecture in a hardware description language and synthesized the circuit using a standard cell library in a 0.18-micron CMOS technology. The size of the circuit is less than 1 mm^2 and the simulated power consumption is less than 250 mW from a supply voltage of 1.8 V.

5. CONCLUSION

In this paper, an impulse-radio UWB system for short-range communication is proposed. A physical layer packet format that ensures accurate timing acquisition in the receiver is first introduced. A baseband receiver architecture is then designed to meet the low-complexity requirement for UWB applications. Simulation results on PER and boundary detection in multipath channel environment show that the proposed system indeed is capable of low-power, short-range wireless communication applications. Finally, the proposed architecture has been mapped to an ASIC implementation with low power consumption and thus can work as a foundation for future single-chip UWB communication transceivers.

6. REFERENCES

[1] M. Z. Win and R. A. Scholtz, "Impulse radio: how it works," *IEEE Commun. Lett.*, vol. 2, no. 2, pp. 36 –38, Feb 1998.

[2] I. O'Donnell, S. W. Chen, B. T. Wang, and R. W. Brodersen, "An integrated, low power, ultra-wideband transceiver architecture for low-rate, indoor wireless systems," in *IEEE CAS Workshop on Wireless Communications and Networking*, Sep 2002.

[3] N. M. Deshpande and G. Borriello, "Location-aware computing: Creating innovative and profitable applications and services," Intel Research and Development, 2002.

[4] "Revision of Part 15 the Commissions rules regarding ultra-wideband transmission systems," FCC ET Docket 98-153, 2002.

[5] S. Budisin, "Golay complementary sequences are superior to PN sequences," in *IEEE International Conference on Systems Engineering*, Sep 1992, pp. 101 –104.

[6] Y. H. Lin, "Design and implementation of an ultra wide band baseband receiver," M.S. thesis, National Taiwan University, 2003.

[7] D. Cassioli, M. Z. Win, and A. F. Molisch, "The ultra-wide bandwidth indoor channel: From statistical model to simulations," *IEEE J. Select. Areas Commun.*, vol. 20, no. 6, pp. 1247–1257, Aug 2002.